



Article

# Tsunami Alert Efficiency in the Eastern Mediterranean Sea: The 2 May 2020 Earthquake ( $M_w$ 6.6) and Near-Field Tsunami South of Crete (Greece)

Gerassimos A. Papadopoulos <sup>1,\*</sup>, Efthymios Lekkas <sup>2,3</sup>, Katerina-Navsika Katsetsiadou <sup>2</sup>, Emmanouil Rovythakis <sup>2,4</sup>  and Amir Yahav <sup>5</sup>

<sup>1</sup> International Society for the Prevention & Mitigation of Natural Hazards, 10681 Athens, Greece

<sup>2</sup> Department of Geology & Geoenvironment, National & Kapodistrian University of Athens, 15784 Athens, Greece; elekkas@geol.uoa.gr (E.L.); knavsika@geol.uoa.gr (K.-N.K.); manolis.royythakis@gmail.com (E.R.)

<sup>3</sup> Earthquake Planning and Protection Organization, 154 51 Neo Psychiko, Greece

<sup>4</sup> Fire Brigade Department, Crete, 72200 Ierapetra, Greece

<sup>5</sup> National Steering Committee for Earthquake Preparedness, Tel-Aviv 61171, Israel; av\_y@hotmail.com

\* Correspondence: gerassimospapadopoulos2@gmail.com; Tel.: +30-2106007533

Received: 1 July 2020; Accepted: 27 July 2020; Published: 30 July 2020



**Abstract:** The Mediterranean tsunami warning system is based on national monitoring centers (Tsunami Service Providers, TSPs) and operates under the IOC/UNESCO umbrella. For the first time we evaluate in depth the system's performance for improving its operational effectiveness in conditions of extremely narrow time frames due to the near-field tsunami sources. At time 10 ( $\pm$  2) min from the origin time,  $t_o$ , of the 2 May 2020 ( $M_w$ 6.6) earthquake in Crete, the Greek, Italian and Turkish TSPs sent alerts to civil protection subscribers. A small tsunami (amplitude  $\sim$ 16 cm a.m.s.l.) of magnitude  $M_t$ 6.8, arriving at south Crete in  $\sim$ 17 min from  $t_o$ , was documented from tide-gauge records and macroscopic observations. The analysis of the upstream alert messages showed that the tsunami alert efficiency is not adequate, since (1) earthquake parameters of low accuracy were used for the initial message, (2) alerts were issued after some forecasted wave arrival times had expired, (3) alert messages are characterized by various discrepancies and uncertainties. Our calculations showed that the upstream component improves if the alert time is shortened by a few minutes and the initial earthquake parameters are more accurate. Very late procedures were noted in the Greek civil protection downstream component, thus rendering response actions useless. In Israel, a bit more time was available to the authorities for decision making. A drastic improvement of the downstream component is needed to achieve timely alerting for local authorities and communities.

**Keywords:** near-field tsunamis; Mediterranean warning system; 2020 earthquake and tsunami; upstream alert component; downstream alert component; tsunami alert efficiency; Crete; Greece; Israel

## 1. Introduction

Near-field tsunamis produced in subduction zones arrive at the closest coasts in tenths of minutes or less [1], thus leaving very little time for early warning. About 80% of victims due to tsunamis worldwide are caused within the first 1 h of tsunami propagation [2]. In the eastern Mediterranean, the Hellenic Subduction Zone (HSZ) marks the convergence lithospheric plate boundary between the Nubian (African) plate and the southern margin of the Eurasian plate where the former subducts underneath the later (Figure 1a). On 2 May 2020 a strong earthquake with a moment magnitude  $M_w = 6.6$  ruptured to the south of Crete, in the Hellenic Subduction Zone (HSZ) (Figure 1a). The earthquake epicenter was located at a distance of  $\sim$ 90 km from the closest coast of Crete, which implies that it was a very near-field source for tsunami generation. According to the alerting protocols adopted within the

frame of the North-East Atlantic and Mediterranean Tsunami Warning System (NEAMTWS) of the Intergovernmental Oceanographic Commission (IOC) of UNESCO, the Tsunami Service Providers (TSPs) in the eastern Mediterranean region issued tsunami warning messages within about 10 min from the 2 May 2020 earthquake origin time.

In the Mediterranean Sea basin, tsunami waves are generated not only by strong submarine or coastal earthquakes, like the 2 May 2020 one, but also by volcanic eruptions and landslides [3,4]. The most active geodynamic structure in the Mediterranean is the arc and trench system of the HSZ, which produces mega thrust tsunamigenic earthquakes [5,6]. Several pre-historical and historical tsunamis have been reported in the Mediterranean region [3–7]. In around 1600 B.C. a large tsunami was produced during the giant eruption at the volcano of Thera (Santorini) in the back-arc region of the Hellenic Arc. Well-known historical examples are the tsunamis of AD 365 and 1303, which were generated by major earthquakes with estimated magnitudes  $M \sim 8.0$ – $8.5$  and propagated up to remote places in the eastern Mediterranean, such as Alexandria and Haifa (Figure 1). In the 20th century two strong and destructive seismic tsunamis were caused in the Messina strait, south Italy, on 28 December 1908, and in the south Aegean Sea, Greece, on 9 July 1956 [3,4]. Although large tsunamis are rare in the Mediterranean, they remain high impact events. Coastal zones of the region are threatened mainly by very near-field tsunami sources. However, in case of basin-wide tsunamis, coastal zones at distances of  $\sim 1$  h of tsunami travel time are also at risk. For example, coasts in the Levantine Sea, e.g., Israel, are threatened not only by local tsunamis but also by remote tsunamis which are generated along the HSZ [8,9]. In the last decade or so, several small tsunamis were detected after strong earthquakes of magnitude  $< 7$  thanks to the tide-gauge networks developed after the establishment of the Intergovernmental Coordination Group (ICG)/NEAMTS (see the Discussion section).

In the North-East Atlantic and Mediterranean (NEAM) region, a systematic and coordinated tsunami risk mitigation program practically started in the aftermath of the Indian Ocean's mega tsunami on Boxing Day 2004. However, the need to develop such a program, including the operation of early warning systems, was stressed well before 2004 thanks to relevant EU-supported tsunami research projects [10,11]. In November 2005 the country members of the IOC/UNESCO established the Intergovernmental Coordination Group (ICG) of the NEAMTWS, which is supported by five national monitoring centers, acting as TSPs, and by several technical Working Groups and Task Teams. The monitoring centers started operations gradually from the summer of 2012. However, NEAMTWS provides services only for seismic tsunamis, leaving aside tsunamis produced by other causes, such as volcanic eruptions and landslides.

After more than five years of real operational experience within NEAMTWS, it is of interest to evaluate the performance of the system. So far the effort for such an evaluation remains quite limited [9]. On 1 July 2009 an earthquake and tsunami similar to that of 2 May 2020 were observed to the south of Crete [12] but the NEAMTWS was not yet operational. More recently, the system's operational evaluation was examined [13] after a local tsunami observed in SE Aegean Sea after a  $M_w = 6.6$  earthquake that ruptured the Bodrum-Kos area on 20 July 2017. On the other hand, so far no information is available on the extent to which the tsunami alert messages reached local communities. However, for the local tsunami that followed, the 2 May 2020 earthquake ( $M_w = 6.6$ ) to the south of Crete in the HSZ, Greece (Figure 1), data are available for both the upstream and downstream components of the warning system, and, therefore, this case offers a good opportunity to evaluate the operational performance of both components. To this aim we present the main observations regarding the 2020 earthquake and tsunami, analyze the operational efficiency of the upstream component of the system based on a series of alert messages issued by three TSPs, examine the downstream component focusing on the civil protection response in Greece and in Israel and discuss realistic perspectives for improving the tsunami alert efficiency.

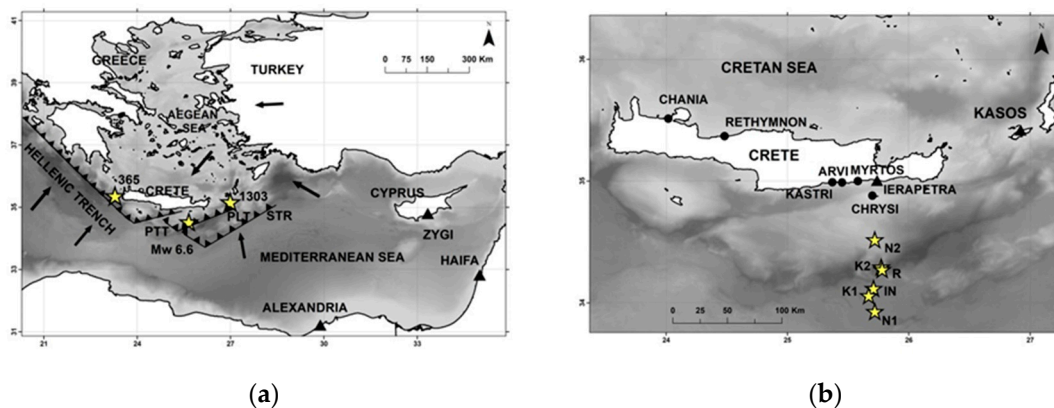


**Figure 1.** (a) Seismotectonic frame of the 2 May 2020 earthquake ( $M_w = 6.6$ ) to the south of Crete. The Nubian lithosphere subducts from the Mediterranean underneath the Aegean Sea at the southern Eurasian plate margin [12]. Arrows and stars show lithospheric plate motions and earthquake epicenters, respectively. The Ptolemy (PTT), Pliny (PLT) and Strabo (STR) trenches, as well as the epicenters of the large historical earthquakes of AD 365 and 1303, are also shown. The tsunami caused by the 2020 earthquake was recorded at two near-field tide-stations (solid triangles in b) as well as at the Alexandria station. No clear wave signal was detected at the Zygi and Haifa stations. (b) Epicenter of the 2 May 2020 earthquake as determined by various institutes: N1, N2 (= NOA1, 2), K1, K2 (= KOERI 1, 2), IN (= INGV), R (= reference epicenter by GFZ, similar to the one determined by USGS); 1,2 stand for initial and updated epicenters, respectively. Acronyms INGV, NOA, KOERI are explained in Section 2.2 and GFZ in Section 2.3.1. The 2020 tsunami was recorded at the Ierapetra and Kasos tide-stations and reported from Arvi, Kastri and Chrysi islet. The 1 July 2009 tsunami was reported from Arvi, Myrtos and Chrysi islet. Solid dots show localities.

## 2. Materials and Methods

### 2.1. Method Overview

We briefly introduce the current architecture of the NEAMTWS as well as the operational upstream and downstream components of the system and the responsibilities of the TSPs. The large earthquake of 2 May 2020 and its associated tsunami are described on the basis of instrumental records and macroscopic observations, while the tsunami magnitude,  $M_t$ , is calculated. Based on the tsunami forecasts contained in the alert messages issued by three TSPs after the earthquake, we examine in depth the tsunami alert efficiency for the first time in the NEAMTWS history. Our analysis included both the upstream alert component and the downstream performance of the tsunami response by the authorities in Greece and Israel. This evaluation has been made in light of the extremely narrow early warning time imposed by the near-field nature of the tsunami source. All times referred to are in UTC unless otherwise noted.

### 2.2. NEAMTWS Operational Architecture

The operational architecture of NEAMTWS is currently based on five TSPs, which are national centers charged with seismic and tsunami monitoring in France (CENALT, Centre d'Alerte aux Tsunamis, Paris, France), Italy (INGV, Istituto Nazionale di Geofisica e Vulcanologia), Greece (NOA, National Observatory of Athens), Portugal (IPMA, Instituto Português do Mar e da Atmosfera) and Turkey (KOERI, Kandilli Observatory and Earthquake Research Institute). The national centers CENALT, INGV, NOA and KOERI obtained international accreditation within the frame of IOC/UNESCO in September 2016 while IPMA's was obtained in December 2019. No responsibility areas have been endorsed by the ICG/NEAMTWS but each TSP has its own competence monitoring area. A country member subscribes to receive tsunami alert messages from one or more TSP(s) on the basis of bilateral agreement(s). Within the upstream component of the system, tsunami alert messages

are issued on the basis of two main elements: instrumental records of the earthquake and of the tsunami, if any, and a Decision Matrix (DM). More information on the NEAMTWS can be found at [http://www.ioc-tsunami.org/index.php?option=com\\_content&view=article&id=10&Itemid=14](http://www.ioc-tsunami.org/index.php?option=com_content&view=article&id=10&Itemid=14).

The earthquake solution is based on national and regional seismograph networks and provides focal parameters of the seismic event, i.e., origin time, earthquake epicenter, focal depth and magnitude usually within ~2–4 min from the earthquake origin time,  $t_0$ . Networks of tide-gauge stations installed at selected near-shore spots record sea level changes. However, no ocean bottom instruments for operational tsunami purposes are available so far in the Mediterranean Sea. Because of the near-field tsunami character and the absence of ocean bottom instruments, the potential generation of a tsunami initially relies on the DM, i.e., a tool composed by a set of empirical rules indicating the possibility for an earthquake to generate a tsunami depending on the values of the focal parameters. The DM also predicts the threat level based on these parameters. The ICG/NEAMTWS endorsed a common DM form but allows each TSP to decide about the specifications of the DM numerical values adopted. An earlier evaluation of the DM's performance in the NEAM region can be found in Ref. [14].

In the Mediterranean region, the DMs in use by the TSPs are similar in their general form, although there are some differences. The tsunami threat level at a particular coastal point scales with the earthquake magnitude,  $M$ , and the epicentral distance,  $d$ . Magnitude  $M$  is the best available to a TSP at the time of the tsunami alert issue. Three threat levels are predicted by the DMs in current use: *Tsunami Information* ( $5.9 \leq M$  or  $6.0 \leq M \leq 6.4$  and  $d \geq 100$  km), *Tsunami Advisory* ( $6.0 \leq M \leq 6.4$  and  $d < 100$  km or  $6.5 \leq M \leq 6.9$  and  $d \geq 100$  km or  $7.0 \leq M \leq 7.4$  and  $d > 400$  km), *Tsunami Watch* ( $6.5 \leq M \leq 6.9$  and  $d < 100$  km or  $7.0 \leq M \leq 7.4$  and  $400 \text{ km} \geq d \geq 100 \text{ km}$  or  $M \geq 7.5$ ). The general features of the threat levels are shown in Table 1. Tsunami alerts are categorized as local ( $d < 100$  km), regional ( $100 \text{ km} \leq d \leq 400 \text{ km}$ ) and basin-wide ( $d > 400 \text{ km}$ ). The above scheme is valid for the DM in use by INGV and KOERI. In the DM which is used by NOAA, however, the characterization of the tsunami threat level is shifted by a lower magnitude range step. For example, for  $5.5 < M \leq 6.0$  at local and regional distances, the threat levels *Advisory* and *Information* are predicted, respectively, while in the range  $6.0 < M \leq 6.5$  the threat level is *Watch* for local distance and *Advisory* for regional distance, and so on.

**Table 1.** Tsunami threat levels and their features as adopted by the Intergovernmental Coordination Group (ICG)/NEAMTWS.

Threat Level	Tsunami Wave	Effects on the Coast
Tsunami Information	No wave expected	No tsunami threat
Tsunami Advisory	Tsunami wave height ranges between about 0.2 m and 0.5 m and/or tsunami run-up < 1 m	Currents, bores, recession, damage in harbors, small inundation on beaches
Tsunami Watch	Tsunami wave height > 0.5 m and/or tsunami run-up > 1 m	Coastal inundation

There are four types of tsunami alert messages: Initial message (I), Ongoing message (O), End message (E) and Cancel message (C). The I-message is the very first alert message that a TSP issues after an earthquake which might cause tsunami, according to the DM. Such a message is based on the very first solution of the seismic event available to a TSP. The O-messages are issued when updated earthquake solutions and/or tide-gauge records are available. The E-messages are issued when TSPs decide that no more information of operational interest is available for dissemination. A C-message is issued in case there is need to cancel the alert procedure, e.g., in case of false alarm. At the current stage of the NEAMTWS development, the tsunami messages issued by the TSPs are not public but are transmitted only to prescribed Civil Protection Authorities (CPAs).

The initial determination of the earthquake focal parameters is of crucial importance for organizing the content of an I-tsunami message immediately after an earthquake event and according to the DM which is applicable. At the current stage of development, the target time endorsed by the ICG/NEAMTWS to issue an I-message is 10 min. The content of an I-message includes the time

and number of the message issued, the focal parameters of the earthquake, the threat level and the respective area threatened, as well as the forecasted wave arrival times at prescribed forecast points.

The tsunami alert messages issued by a TSP are transmitted via e-mail, fax machines and GTS (Global Telecommunication System) to subscribed national CPAs of the IOC country members, to other TSPs, to IOC/UNESCO, as well as to the ERCC (Emergency Response Coordination Center) of the European Commission in Brussels (Figure 2).

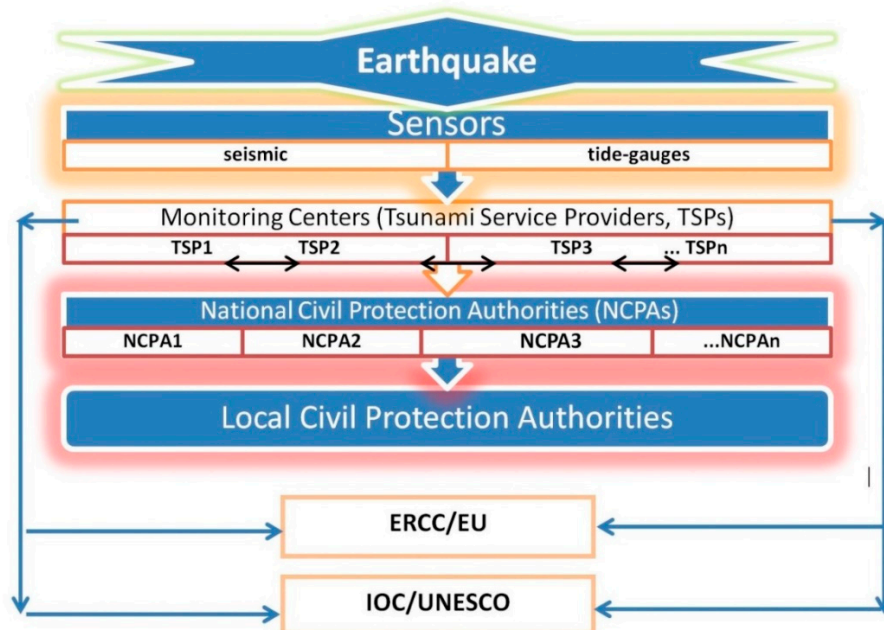


**Figure 2.** Flow chart of the North-East Atlantic and Mediterranean Tsunami Warning System (NEAMTWS)/Intergovernmental Oceanographic Commission (IOC)/UNESCO operational architecture. The upstream component of the system includes the steps until the alert messages are sent to National Civil Protection Authorities. The next steps of the procedure compose the downstream component.

### 2.3. The 2020 Earthquake and Tsunami Event

#### 2.3.1. Observations

On 2 May 2020, at 12:51:06.5 UTC, a shallow strong earthquake ruptured offshore to the south of Crete, at the central segment of the HSZ (Figure 1). The initial magnitude of  $M_w = 6.6$  and hypocenter ( $25.75^\circ$  E/ $34.27^\circ$  N,  $h = 10$  km) determined by the GEOFON network of the Deutsches GeoForschungsZentrum (GFZ) (<https://geofon.gfz-potsdam.de/>) have been considered as reference parameters for our analysis, since they are consistent with the determinations of other centers, e.g., USGS (<https://earthquake.usgs.gov/earthquakes/search/>). The 2 May 2020 earthquake was perceptible in various places of Crete and beyond, but no damage was reported.

Soon after the earthquake, local authorities and eyewitnesses reported a tsunami wave observed along the coast of the southeastern side of Crete. The tsunami has been documented in a series of pictures and video shootings taken by local authority persons, by the press as well as by amateurs at coastal spots of the Ierapetra town, at the nearby villages of Arvi and Kastri as well as at the northern side of Chrysi islet (Figure 1b, Figure 3, Figure 4 and Appendix A). From eyewitness accounts it results that the tsunami of 2 May 2020 was similar to the one reported after the earthquake of 1 July 2009. The 2009 tsunami was observed at Arvi and Myrto villages as well as at the north side of Chrysi islet (Figure 1b) [12]. No tide-gauges were operating in the area in 2009. However, a video record that documented the strong water flow in the harbor of Arvi has been collected by us.



**Figure 3.** (a) Sea retreat and (b) sea level oscillation by ~25 cm at the Ierapetra port, southeastern Crete, observed a few minutes after the 2 May 2020 earthquake (photo courtesy of Mr. Emmanouil Rovythakis).

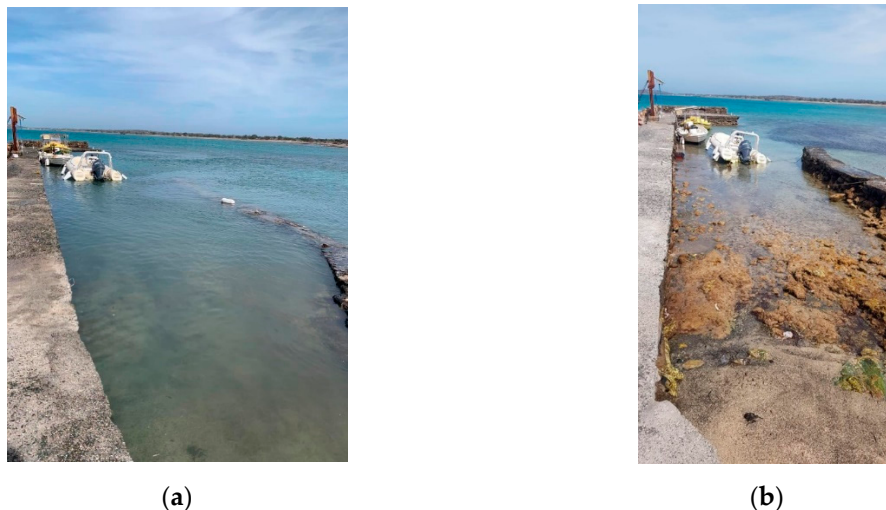


**Figure 4.** (a) The small port at the north side of Chrysi islet before the 2 May 2020 earthquake, and (b) sea level drop by ~35 cm and boats stranded as if on dry land after the earthquake (photo courtesy of Mr. George Garefalakis).

From the observational material collected, it is evident that the 2 May 2020 tsunami appeared as a series of relatively short-period oscillations and strong water currents. The maximum sea level rise and drop was macroscopically estimated at ~25 cm at Ierapetra and at ~30–35 cm in Chrysi islet. No damage was reported from the tsunami. The 2020 tsunami has also been documented on the tide-gauge records of the Ierapetra (NOA-04) and Kasos (NOA-03) stations and situated at epicentral distances of  $\Delta \sim 90$  km and  $\Delta \sim 180$  km, respectively (Figure 1b). In Ierapetra station, south Crete, Greece, the sea water disturbance initiated at ~13:07 with a likely retreat of the water. This is consistent with several eyewitness accounts. A peak amplitude of  $A \sim 0.16$  m was recorded at 13:16 (Figure 5). Taking the crest-to-trough values of  $A$  for three sequential oscillations recorded from 13:12 to 13:18, we obtained once again an average maximum value of 0.16 m and a wave period of  $T \sim 3.5$  min. In Kasos station, SE Aegean Sea, Greece, the record showed a first sea water disturbance, likely water rise, at ~13:39. A peak amplitude of  $A \sim 0.05$  m was recorded at 13:54 (Figure 6), while the wave period was found at  $T \sim 8$  min. In Alexandria tide-gauge station IDSL-23, situated at  $\Delta \sim 485$  km to the southeast of the epicenter (Figure 1) and operated by the National Institute for Oceanography and Fisheries (NIOF), Egypt, a weak tsunami signal has been recorded with an amplitude of 0.02–0.03 m at time ~14:27

(Figure 7). The inspection of the tide-gauge record at the station Zygi Marina, Cyprus, situated at  $\Delta \sim 670$  km to the east (Figure 1), showed no clear tsunami signal.

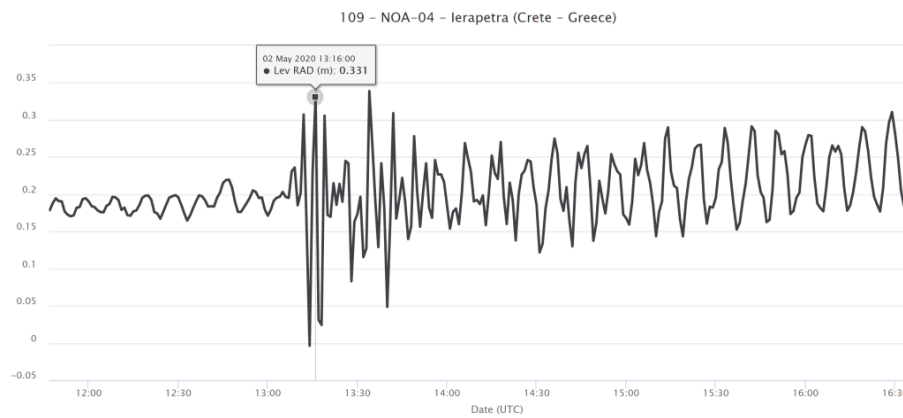


Figure 5. Tsunami record at Ierapetra NOA-4 station.

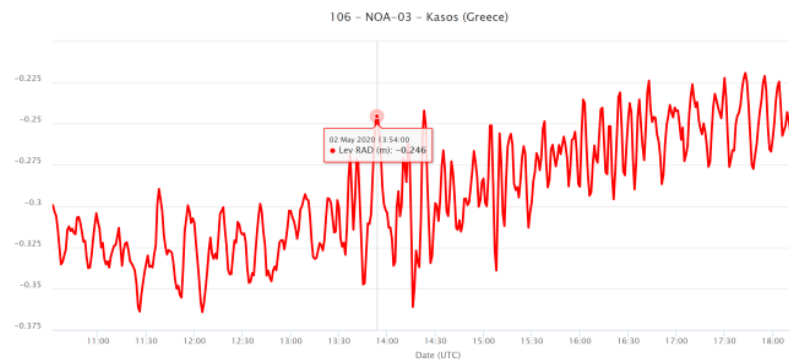


Figure 6. Tsunami record at Kasos NOA-3 station.



Figure 7. Tsunami record at Alexandria station.

### 2.3.2. Tsunami Alert Data

Soon after the 2 May 2020 earthquake generation, the TSPs of INGV, KOERI and NOA produced respective I-alert messages based on the very first solutions of the seismic event available to each TSP. O-messages were issued when updated earthquake solutions and tsunami records were obtained. The time line of the I-, O- and E-messages issued are summarized in Table 2. Ierapetra town and nearby

villages are the settlements situated closest to the earthquake source and, therefore, they have been the coastal spots with the shortest forecast times.

**Table 2.** Time line of upstream tsunami alerts issued by the Tsunami Service Providers (TSPs) of the Istituto Nazionale di Geofisica e Vulcanologia (INGV), National Observatory of Athens (NOA) and Kandilli Observatory and Earthquake Research Institute (KOERI) after the earthquake of 2 May 2020. End messages were issued at 17:50 (KOERI), 17:56 (NOA), 17:59 (INGV). Earthquake reference parameters are from the Deutsches GeoForschungsZentrum (GFZ). Key:  $t_o$  = earthquake origin time, I = Initial message, O = Ongoing message;  $M_w$  = moment magnitude, \* shows local magnitude ( $M_L$ ),  $\varphi^\circ\text{N}$  and  $\lambda^\circ\text{E}$  = epicentral coordinates,  $\Delta$  = epicentral distance,  $h$  = focal depth;  $t_A$  = record time of amplitude  $A$  (maximum peak a.m.s.l.) in Ierapetra tide-gauge station. Threat level: W = Watch, A = Advisory. Forecast points: F1 = Gavdos-Karave, F2 = Ierapetra, F3 = Chora-Sfakion, F4 = Karpathos-Mesochori, np = not provided. All times are in UTC.

Institutes/Actions	Issue Time	Alert	$M_w$	$\varphi^\circ\text{N}$	$\lambda^\circ\text{E}$	$\Delta$ (km)	$h$ (km)	$t_A$	$A$ (m)
Earthquake reference parameters									
GFZ	$t_o = 12:51:06$		6.6	34.27	25.75	90	10		
Upstream alert messages									
INGV-I	12:59	13:10/F1A 13:12/F2W 13:12/F3A	6.7	34.12	25.71	105	20		
NOA-I	13:02	13:07/F2A 13:12/F1A	6.0 *	33.93	25.72	120	10		
KOERI-I	13:03	13:07/F2A 13:11/F1A	6.7	34.06	25.67	110	10		
INGV-O	13:21	As in INGV-I	6.7	34.12	25.71	105	20	13:16	0.13
NOA-O	13:27	13:00/F2W 13:11/F3W	6.5	34.52	25.72	55	15	13:16	0.14
KOERI-O	13:35	W (np)	6.7	34.28	25.74	85	28.7	13:16	0.14
INGV-O	13:50	As in INGV-I	6.7	34.12	25.71	105	20	13:34	0.15

### 3. Results

#### 3.1. Tsunami Size

In contrast to the progress noted with the establishment of gradually improving earthquake magnitude scales, such as the scales of local magnitude,  $M_L$  [15], surface-wave magnitude,  $M_s$  [16], and moment magnitude,  $M_w$  [17], no standard tsunami magnitude scales have been introduced so far. However, several attempts have been made since the 1940s see review in Ref. [18], one of the most promising being the method introduced by Abe [19]. For this reason, tsunami intensity has been used for several years as a proxy of tsunami size, yet it is a useful tool to estimate the event impact. Here, we estimate both the intensity and the magnitude of the 2 May 2020 tsunami.

Earlier tsunami intensity scales were of only six grades see review in Ref. [18]. A new, widely adopted 12-grade tsunami intensity scale, that followed the tradition of the 12-grade macroseismic intensity scales, was introduced in 2001 [20]. Based on the new scale, we estimated a tsunami intensity level of grade 4 for both the 2020 and 2009 local tsunamis.

A promising tsunami magnitude scale is based on Pacific Ocean data and uses formula (1) to calculate tsunami magnitude,  $M_t$ , from the maximum wave heights,  $H$  (in m), at near-shore tide-gauge records at epicentral distances,  $\Delta$  (in km) [19]:

$$M_t = \log_{10} H + \log \Delta + 5.80 \quad (1)$$

This formula is similar to the one introduced [16] for the calculation of  $M_s$ . The constant in (1) was obtained by requiring  $M_t = M_w$  on the average for the calibration data set [19]. The dependence of  $M_t$  on  $\log_{10} H$  was based on the empirical relation between  $M_w$  and  $\log_{10} H$ . Then, the tsunami amplitude

scales with the event size.  $M_t$  represents not only the overall physical size of a tsunami but also the seismic moment of the tsunamigenic earthquake.

In the Mediterranean Sea basin, the applicability of formula (1) was tested for the first time very recently [18], after the earthquake ( $M_w = 6.8$ ) of 25 October 2018 that ruptured the western segment of the Hellenic arc. From five tide records it was found that  $M_t = 7.0$ , which is a good approximation to  $M_w = 6.8$ , calculated from seismic records. The above procedure was applied to the 2 May 2020 tsunami wave. From the tsunami records at Ierapetra ( $H = 0.16$  m;  $\Delta = 90$  km), Kasos ( $H = 0.05$  m;  $\Delta = 180$  km) and Alexandria ( $H = 0.025$  m;  $\Delta = 485$  km), we obtained an average  $M_t = 6.87$ , which is also close to the seismic moment magnitude  $M_w = 6.6$ .

### 3.2. Upstream Alert

#### 3.2.1. Tsunami Messages

The various tsunami messages are organized on the basis of the earthquake focal parameters, on the DM adopted by a TSP as well as on the tsunami records available, if any. The three I-messages issued were based on the adoption of three different initial seismic solutions (Table 2), which are characterized by two main differences. First, the magnitude  $M_L = 6.0$  used by NOA was significantly underestimated with respect to  $M_w = 6.7$ , used by INGV and KOERI. A few minutes later, NOA adopted  $M_w = 6.5$  and used it in its O-message. Second, the initial solutions by both NOA and KOERI put the earthquake epicenter to the south of Ierapetra but at a larger distance with respect to that adopted by INGV (Table 2, Figure 1b). These two features had important operational consequences, as analyzed later.

The INGV I- and O-messages were based on the same earthquake solution (Table 2) and forecasted a *Watch* threat level for Ierapetra and *Advisory* level for other, more remote forecast points. Since the INGV earthquake solution did not change, the forecast times remained identical with the ones in the I-message. In the two O-messages released by INGV, additional information of operational interest was incorporated, namely the tsunami amplitude  $A = 0.13$  m recorded at Ierapetra station at time 13:16. The first O-message was issued 13 min after the initiation of the wave in the tide record. A second O-message was released by INGV, slightly updating the tide-gauge parameters (Table 2). However, this message was of low operational value, for it was issued at a late time and contained practically no new information with regard to the first INGV O-message.

For the town of Ierapetra, the NOA I-message indicated a lower threat level with respect to that of INGV, i.e., *Advisory* against *Watch*. Later, NOA adopted the revised magnitude  $M_w = 6.5$  and epicentral distance for Ierapetra  $\Delta \sim 55$  km, instead of  $\Delta \sim 120$  km (Table 2). Consequently, with the O-message of NOA, the threat level was upgraded to *Watch*. However, the consequence of the change in earthquake parameters has been to change most of the travel times forecasted, which have thus become different not only from the INGV forecasts but also with respect to the initial forecasts listed in the NOA I-message. Most of the forecast times in the O-message of NOA shifted earlier from 7 min to 20 min with respect to the times for the same forecast points in the I-message (Figure 8). The average shift was found equal to  $-4.1 (\pm 4.12)$  min. Only one forecast time did not change, while only two shifted a bit later by 1 and 2 min. Such differences issued in a short time interval may cause confusion to decision-making authorities.

Like NOA, the KOERI TSP initially adopted a seismic source at  $\Delta \sim 110$  km to the south of Ierapetra, but with magnitude  $M_w = 6.7$ , which is coincident with the one used by INGV. Because of the long epicentral distance, however, the initial threat level was *Advisory*. The KOERI I-message was also accompanied by three maps as enriched products of the wave forecasting described in the message itself. Although the number of maps could be reduced to two or even to only one, this material is operationally useful, since it illustrates in an understandable way the overall tsunami threat forecasted. It is of importance for the TSPs to collect responses from message subscribers in order to better understand how such enhanced products meet the operational needs of the subscribers and what are the possible improvements proposed. With its O-message, KOERI adopted a revised earthquake

solution with  $\Delta \sim 85$  km (Table 2) and, therefore, upgraded the threat level from *Advisory* to *Watch*. The KOERI O-message also included parameters from the Ierapetra tide-gauge record consistent with the parameters inserted by INGV and NOA.

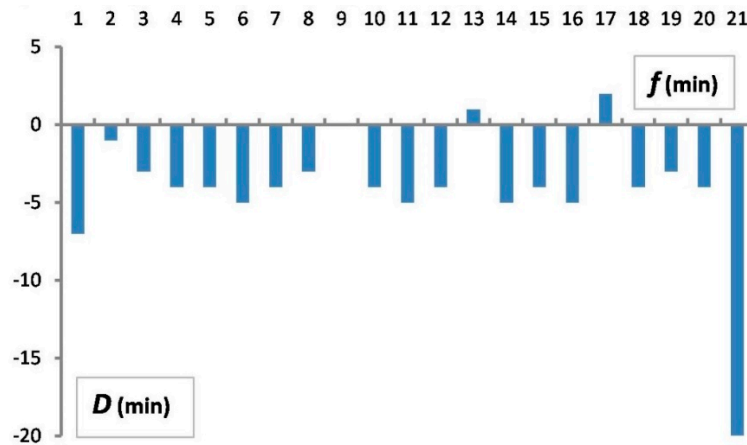


**Figure 8.** Difference  $D = f(I) - f(O)$  of forecast times in the NOA I- and O-messages vs.  $f$  for the same forecast points. Nearly all  $D$ -values are negative, implying that  $f$  times in O-message are systematically shorter as compared to  $f$  times in I-message.

It is noteworthy that none of the O-messages issued by the three TSPs included macroscopic information about the tsunami that was already observed in the coastal zone of southeast Crete. There is no doubt that because of the extreme press for time the TSPs were unable to collect, cross-check and verify macroscopic information that might have been incorporated in their O-messages. Nevertheless, it is of operational interest to investigate if this kind of information, when available in real time and after cross-checking for reliability, could be operationally useful for inclusion in the messages regardless of whether tide-gauge records are available or not.

### 3.2.2. Tsunami Alert Efficiency

According to the standard operational procedures, the I-messages were sent by the three TSPs to their subscribers within an average time  $\tau = 10 (\pm 2)$  min from  $t_o$  (Table 2). Time  $\tau$  is equal to the target time for issuing the I-message adopted by the ICG/NEAMTWS at the current stage of the system's development. In the I-messages, the times forecasted for the first wave arrivals at the closest forecast points in south Crete fit well enough the first wave onset at Ierapetra station. The three I-messages were sent to their subscribers within 5 to 9 min before the first wave arrival at Ierapetra town. This time lag is extremely short, since it leaves only a few minutes for operational decisions and actions in the downstream component of the system.

The issue time of O-messages ranged between 30 and 44 min from  $t_o$  and between 11 and 33 min after the shortest forecast times (Table 2). The last time lag leaves no room for effective operational actions. The three E-messages were issued within a narrow time window of  $\sim 9$  min and about five hours after  $t_o$ .

From the previous analysis, it results that there are four critical times in the upstream component of the warning system in very near-field conditions, such as the ones of the 2 May 2020 tsunami. Suppose that  $t$  is the issue time of an alert message and  $f$  is the forecast time for the first wave arrival at a given forecast point. Then, the four critical times are the issue times of the I- and O-messages,  $t(I)$  and  $t(O)$ , and the respective forecast times,  $f(I)$  and  $f(O)$ , for a given forecast point. Since  $f$  counts from  $t_o$ , of great operational interest is the remaining time from  $t$  to  $f$ , i.e., the differences  $f(I) - t(I)$  and  $f(O) - t(O)$ . The sooner the alert message is issued the larger the remaining forecast time. If the O-message inserts different earthquake focal parameters with respect to those introduced in the I-message, then time  $f(O)$

may change at least for some, if not for all, of the forecast points, as already noted regarding the NOA messages after the 2 May 2020 earthquake.

We introduce the concept of tsunami alert efficiency,  $F$ , as

$$F = (f - t)/f \tag{2}$$

The parameter  $F$  is an indicator of the forecast time percentage remaining after time  $t$ . As an instance,  $F = 0.5$  means that only half of the forecast time remains for a particular forecast point after an alert issue. Theoretically,  $F = 1$  if the I-message is issued simultaneously with the earthquake at time  $t_0$ .  $F$  takes not only positive but also negative values, and this really happens if  $t > f$ , i.e., when the alert message is issued after a forecast time has expired. We compared the parameter  $F$  for the forecast times inserted in the alert messages issued by the three TSPs after the 2 May 2020 earthquake. In the INGV's I- and O-messages, the forecast times for each forecast point remained the same because the same earthquake focal parameters were adopted in the two messages. On the contrary, the earthquake parameters adopted in NOA's O-message are different from the ones in the I-message. For KOERI, only the I-message contained forecast times.

Tsunami alert efficiency curves obtained for the I-messages of the three TSPs (Figure 9) are quite similar but have an apparent shift because the messages were issued at times  $t = 8$  min (INGV),  $t = 11$  min (NOA) and  $t = 12$  min (KOERI) after  $t_0$ . However, a difference in the alert issue of just a few minutes returns a considerable difference in the alert efficiency parameter. In the forecasts of NOA and KOERI, for time  $f$  up to ~20 min the parameter  $F$  takes values less than 0.45 or even less than 0.3. However,  $F$  is ~0.6 in the forecasts of INGV, implying better alert efficiency. Much worse is the alert efficiency obtained for both the INGV's and NOA's O-messages. For time  $f$  up to ~30 min, the parameter  $F$  is negative, which means that for this time range the O-messages were issued after the forecast times for several forecast points had already expired. Again, however, the overall alert efficiency of INGV is better than the one of NOA due to a time difference of 6 min in the issue of the O-messages. There is no doubt that the efficiency would be worst for the KOERI O-message if forecast times were inserted, since the message was issued 8 min after the one by NOA.

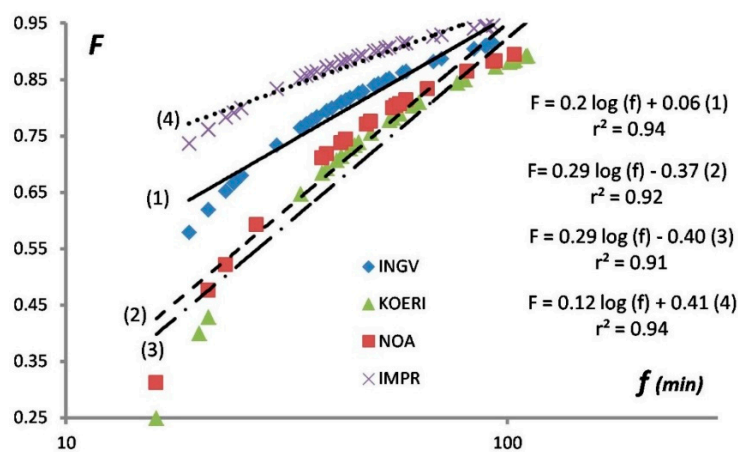


**Figure 9.** Tsunami efficiency curves and respective equations for the I-messages of INGV (1), NOA (2) and KOERI (3);  $f$  is forecast time;  $F$  is tsunami efficiency alert parameter determined from formula (2) in text;  $r$  is correlation coefficient. IMPR (4) is the expected improvement if the I-message was issued only 5 min from the earthquake origin time  $t_0 = 0$  (see Discussion).

### 3.3. Downstream Alert

#### 3.3.1. Greece

In Greece, as soon as the national Operational Center for Civil Protection (OCCP) receives a tsunami message from NOA, TSP initiates the response mechanism by forwarding the message to sectorial emergency centers, e.g., Fire Brigade, Police etc., including the Operational Center for Port Authorities (OCPA). The duty of the sectorial emergency centers is to forward the message further downward. Here, we highlight the actions undertaken in the Greek downstream component of the system after the 2 May 2020 earthquake.

Following the message transmission flow explained above (Figure 2), the OCCP transmitted NOA's message at OCPA, which forwarded it to various Port Authorities in Crete and elsewhere in southern Greece. We have no complete picture of the actions undertaken by all the Port Authorities that received the alert. However, it has been possible to track details of the message flow from the central level up to the Port Authorities of Chania and Rethymnon, two of the most important coastal cities in Crete (Figure 1b).

The Chania Port Authority released an emergency signal directed to local authorities and to the local maritime community in its competence area at 15:38. The emergency, however, was not disseminated to the general population. According to the INGV's I- and O-messages, the forecasted first wave arrival at Chania was 13:41, which is close to the 13:45 forecasted by the I-message of KOERI. The I- and O-messages of NOA, however, forecasted arrival times at 14:12 and 14:14, respectively. This time difference is considerably high from a geophysical and operational point of view, and may reflect important differences in the tsunami propagation models and possibly in the bathymetry files which are in use by the three TSPs. Whatever the possible explanation, this time difference introduces an additional discrepancy between the tsunami messages issued by different monitoring centers and increases the uncertainties in the operational tsunami forecasting. A similar procedure was followed for setting up emergency in the nearby city of Rethymnon. The tsunami arrival times forecasted with the NOA's I- and O-messages have been 13:50 and 13:46, respectively, and are consistent with the ones forecasted by INGV (13:44) and KOERI (13:48). In this case, the emergency signal was released by the Port Authority of Rethymnon at 17:35.

The procedures of emergency at Chania and Rethymnon cities are judged as being extremely late for an effective operational action. On the other hand, however, it is encouraging that the civil protection mechanism was mobilized and responded at the local level even with considerable delay. This is promising for a better performance in the future, given that no relevant action was undertaken by local authorities in past events, e.g., in response to the 1.5 m-high tsunami initiated by the 20 July 2017 earthquake ( $M_w = 6.6$ ) in the SE Aegean Sea [13,21].

It has been documented that local people in Ierapetra and Arvi approached the beach to observe the sea level changes after the earthquake. Although people gathering happened in no massive scale, one may assume that it would be more massive in other circumstances, which may include (i) a higher level of seismic intensity felt in Crete, if either the earthquake source was closer to the island or the magnitude was higher, (2) earthquake incidence in peak summer season, and (3) the absence of COVID-19 social distancing restrictions. Soon after, however, local authorities in Ierapetra decided to keep people away from the beach, although this did not happen in Arvi.

#### 3.3.2. Israel

According to the instructions by the Israeli National Doctrine for Tsunami Preparedness and Response [22,23], in case of an immediate potential tsunami threat, the Tsunami Watch Team (TWT), i.e., the national monitoring center, should approach the Lighthouse Team, which is the senior decision-making team responsible to decide whether or not to alert the country. The release of a national tsunami alert from the Lighthouse Team implies a series of emergency actions along the coast: the evacuation of hundreds of thousands of people who live or work in the area or are enjoying

their vacation, the shutdown of Israel's coastal power plants, setting up an emergency status and the evacuation of seaports, as well as the shutdown and evacuation of industry. Therefore, for Israel, a tsunami alert is a dramatic event, which implies a dramatic decision.

Regarding the earthquake of 2 May 2020, the Israeli coastline was at an epicentral distance of ~840 km. The I-type messages issued by the three TSPs were received a few minutes after time  $t_0$ , e.g., the NOA I-message was received at 13:02 UTC (16:02 local time), i.e., 11 min after  $t_0$ . The alert level was *Information* and, therefore, the operational decision was to continue monitoring the event but to do nothing about the alert. O-messages released by INGV and KOERI did not change the alert level status for Israel. However, the NOA O-message, received by the TWT at 13:27, was a "game changer", because it put Israel at the *Advisory* alert level and forecasted that the first potential tsunami wave arriving at 14:33 would hit Israel's coast near the city of Haifa, a settlement of 284,000 residents and of major seaport and large petrochemical industry. The message arrived 36 min after  $t_0$ , allowing only 1 h and 3 min before the first forecasted tsunami wave arrival. From operational point of view, it is a short time to decide whether to alert or not and to issue an effective early warning.

About 43 min later, i.e., 23 min before the potential hit, the final decision of TWT was to "close" the event after taking into account that only a minor wave had actually been recorded. Otherwise, the time interval of only 23 min would be too short for the Lighthouse Team to make such an important decision, in view of the intrinsic uncertainties involved in the tsunami messages and the high probability to produce a false alarm with many negative economic and social consequences. However, if a higher wave amplitude had been recorded, it would certainly have been preferable to transfer the information to the Lighthouse Team, leaving them to make a decision which could save lives. In any case, the time left to Israeli authorities for decision making was certainly longer with respect to the extremely short time available to the Greek authorities for responding effectively to the tsunami alert.

#### 4. Discussion

The findings of our examination should be seen under the light of the extremely limited time available for an efficient tsunami alert for both the upstream and downstream components of the Mediterranean tsunami early warning system. Although the initial tsunami alert messages were issued by three TSPs with a difference of 1 to 4 min from each other, such a difference is important from an operational point of view. Differences in the alert levels and in the forecast times are due to the use of different DMs, tsunami modeling tools and earthquake parameters and possibly to different bathymetry databases. The main issue with the Mediterranean Sea warning system, however, remains the very near-field character of the tsunami sources. In the eastern basin, several tsunamis were generated after strong earthquakes in the past. However, the accurate record of the tsunami wave arrival times has not been possible due to the lack of appropriate recording means. Tide-gauge networks were deployed after the establishment of the NEAMTWS. On the other hand, the use of video records for tsunami documentation is increasingly popular. Several local tsunamis were generated after strong earthquakes ( $M_w > 6$ ) and recorded thanks to several recording means. In all cases, the first tsunami arrivals were noted in ~30 min or less: Crete ( $M_w = 6.5$ ), 1 July 2009 [12]; Lesvos ( $M_w = 6.3$ ), 12 June 2017 [24]; Bodrum-Kos ( $M_w = 6.6$ ), 20 July 2017 [13,21,24]; Zakynthos ( $M_w = 6.8$ ), 25 October 2018 [18,25]; Crete ( $M_w = 6.6$ ), 2 May 2020 (present study). Such moderate tsunamigenic earthquakes are quite challenging to test and calibrate the capabilities of the tsunami early warning system [12]. Nevertheless, questionnaire surveys among local populations in Greece and Italy showed that people's tsunami risk perception is still low [26,27].

The need to minimize the alert time in both the upstream and downstream components of the tsunami early warning system in the Mediterranean is very urgent. As for the downstream component, it is up to Greece's central and local civil protection authorities to significantly improve the organization of their emergency plans and to find out the optimum technological and operational features for the on-time transmission of early warning messages to local target communities. Such an effort certainly should include and emphasize actions aiming to improve the public's tsunami awareness. It is

disappointing that after a strong submarine earthquake people gather along the seashore to observe the sea level changes, as happened after the 2 May 2020 event.

To further examine the possible improvement of the upstream component efficiency, we considered it absolutely realistic to set up at 5 min the target time to issue I-messages of alert. This has been achieved at least once, e.g., by the NOA TSP after the earthquake ( $M_w = 6.5$ ) in the Ionian Sea on 17 November 2015. Then, the tsunami alert efficiency,  $F$ , for the I-message is significantly improved by a factor of 0.22 to 0.30 (Figure 9). On the other hand, the improvement of the tsunami alert efficiency, mainly for the O-message, is expected by densifying the tide-gauge network with the installation of additional recording devices in critical coastal spots. For example, the installation of new stations in the Crete area would improve the upstream tsunami alert efficiency for tsunami sources like the ones of 2009 and 2020. In spite of the low resolution of the bathymetry grid, tsunami simulations were performed in the area with synthetic tide-gauge networks, two of them installed at the north side of Chrysi islet (Figure 1b) [12]. Those simulations indicate that the time of the first tsunami record could be shortened by  $\sim 3$  min. In that case,  $F$  would improve by a factor of 0.14 to 0.24 (Figure 10).

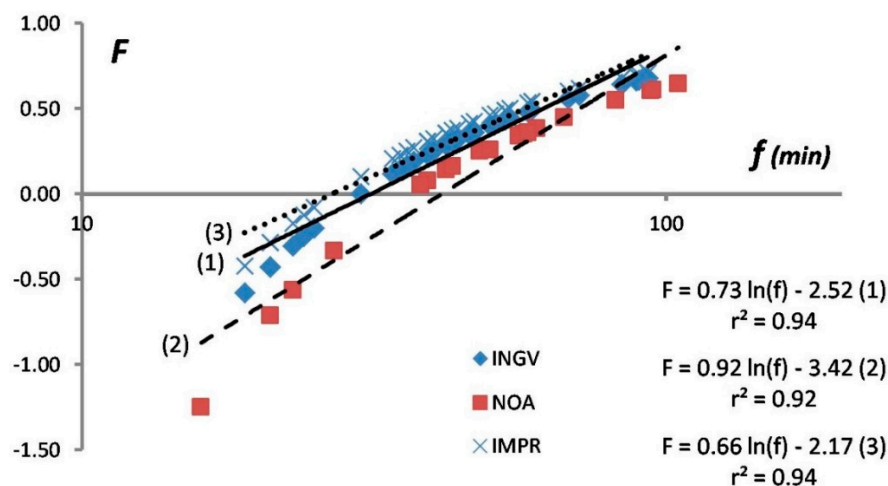


**Figure 10.** As in Figure 9 for the O-messages of INGV (1) and NOA (2), IMPR (3) is the expected improvement if the issue time of O-message is shortened by  $\sim 3$  min thanks to the hypothetical operation of a tide station at Chrysi islet.

Of interest to tsunami service providers are also the operational consequences of the establishment in the Mediterranean region of a well calibrated tsunami magnitude scale,  $M_t$ , since it may provide a new tool for the tsunami wave heights expected in near-field forecasting points as soon as the earthquake magnitude has been determined. Such a prospect was already noted several years ago [28]. However, the utilization of tsunami height/amplitude offshore near the source and in real time conditions becomes of crucial importance. The reason is that one may take into account the need for noise reduction as well as the dynamic effects of the fault on the sea surface and bottom [18].

At the current stage of development of the Mediterranean tsunami warning system, no wave amplitude is forecasted for each of the forecast points. As an alternative, the alert messages indicate the threat level at each point, and this characterization is connected with the wave amplitude range, as shown in Table 1. In the tsunami alert messages issued on 2 May 2020, the threat levels in general are consistent with the observations, although for a few forecast points the *Watch* characterization overestimated the observations, given that no wave exceeding 0.5 m in amplitude was observed. The criteria to determine the point of time to end the tsunami alert procedure is still under discussion within the ICG/NEAMTWS. However, practically speaking, the TSPs usually allow enough time to ensure that the tsunami threat has gone before they issue E-messages. This was also the case on 2 May 2020.

## 5. Conclusions

The Mediterranean Sea basin is characterized by very near-field tsunamis, with the shortest wave travel times being, as a rule, of less than 30 min. After the strong earthquake ( $M_w = 6.6$ ) on 2 May 2020 in Crete, Greece, a small, non-damaging tsunami was macroscopically observed in the town of Ierapetra and in nearby villages on the southeastern coast of Crete. The wave was also recorded by tide-gauge stations in Ierapetra at SE Crete (epicentral distance  $\Delta \sim 90$  km), in Kasos ( $\Delta \sim 180$  km), SE Aegean Sea, and in Alexandria ( $\Delta \sim 485$  km), Egypt. The largest wave amplitude of 0.16 m a.m.s.l. was recorded at Ierapetra station. We estimated that the tsunami was of intensity 4 in the 12-grade tsunami intensity scale [20,29] and of magnitude 6.87 in the  $M_t$  scale [19], which is close to the seismic moment magnitude  $M_w = 6.6$ .

An in-depth analysis of the tsunami early warning issued by three TSP monitoring centers that support the upstream component of the warning system in the eastern Mediterranean showed that, at the current stage of development, the system does not provide timely and efficient alerts. The earthquake origin time was 12:51 UTC, while the first alert was issued at 12:59 and the first wave arrival was recorded at 13:07. The tsunami alert efficiency,  $F$ , i.e., the percentage of the remaining forecast time after the issue time of the initial alert message, was less than 0.6, or even less than 0.3 for several forecast points. The situation is worst as regards the issue time of the first ongoing alert message (13:21), since  $F$  becomes negative for several forecast points. The reason is that the message was issued after the forecast time had expired for those points. Based on previous tsunami wave simulations in the same area [12], we judged that the tsunami alert efficiency could be improved if the issue time of alert messages is shortened by a few minutes, which is an absolutely realistic goal.

Inconsistencies between the initial earthquake parameters adopted by the three TSPs caused important operational consequences. We showed that the initial earthquake parameters adopted are of crucial operational importance and that the adoption of revised parameters in an ongoing message is seismologically acceptable but creates serious operational problems. Therefore, TSPs should drastically improve the accuracy of the initial magnitude and location of the earthquake event, to avoid revising ongoing messages within a very short time.

In the downstream component of the warning system, the response of the national and local Greek civil protection authorities was too slow and practically rendered useless from an operational point of view. However, even the delayed response is encouraging, since in previous events no response was noted at the local level. The authorities should drastically improve their response system and intensify tsunami awareness programs for the general public. In Israel, the authorities had a bit more time to decide that there was no need to set up a tsunami emergency for the coastal zone of the country. In any case, the event was a challenging test of the Mediterranean tsunami warning system in real conditions.

**Author Contributions:** Conceptualization and methodology, G.A.P.; software, G.A.P., K.-N.K.; validation, K.-N.K. and E.R.; resources and data curation, G.A.P., K.-N.K., E.R., A.Y.; writing—original draft preparation, G.A.P., A.Y.; writing—review and editing, E.L., K.-N.K., E.R., A.Y.; supervision, G.A.P. All authors have read and agreed to the published version of the manuscript.

**Funding:** This research received no external funding.

**Acknowledgments:** The tsunami tide-gauge records at stations NOA-03 and NOA-04 (Greece) and NIOF-IDSL-23 (Egypt) were collected from the database of the Space, Security and Migration Directorate-JRC Ispra, EU (<https://webcritch.jrc.ec.europa.eu/SeaLevelsDb/Home>). Thanks are due to Sergiu Dov Rosen, Haifa, Israel, for a useful discussion regarding the tsunami records. The recommendations of three anonymous reviewers aiming to improve the initial paper submission were greatly appreciated.

**Conflicts of Interest:** The authors declare no conflicts of interest.

## Appendix A

Video shootings showing the 2 May 2020 tsunami at Ierapetra coast.

- <https://www.facebook.com/maria.roumeliotakiskyvalou/videos/pcb.2799497790335638/2799492307002853/?type=3&theater;>

- <https://www.facebook.com/maria.roumeliotakiskyvalou/videos/pcb.2799497790335638/2799492307002853/?type=3&theater;>
- [https://www.facebook.com/maria.roumeliotakiskyvalou/videos/pcb.2799497790335638/2799496940335723/?type=3&theater.](https://www.facebook.com/maria.roumeliotakiskyvalou/videos/pcb.2799497790335638/2799496940335723/?type=3&theater;)

Video shootings documenting the 2 May 2020 tsunami at Arvi coast.

- [https://www.youtube.com/watch?v=9Qobru4\\$\times\\$4WQ&feature=youtu.be;](https://www.youtube.com/watch?v=9Qobru4$\times$4WQ&feature=youtu.be;)
- [https://www.facebook.com/100001618268477/videos/3088854047845174/;](https://www.facebook.com/100001618268477/videos/3088854047845174/)
- <https://www.youtube.com/watch?v=ePnn4g64LeM&feature=youtu.be;>
- [https://www.youtube.com/watch?time\\_continue=1&v=0JrdCBKssn8&feature=emb\\_logo.](https://www.youtube.com/watch?time_continue=1&v=0JrdCBKssn8&feature=emb_logo.)

## References

1. Tsushima, H.; Kenji, H.; Yutaka, H.; Tanioka, Y.; Kimura, K.; Sakai, S.; Shinohara, M.; Kanazawa, T.; Hino, R.; Maeda, K. Near-field tsunami forecasting using offshore tsunami data from the 2011 off the Pacific coast of Tohoku Earthquake. *Earth Planets Space* **2011**, *63*, 821–826. [[CrossRef](#)]
2. Gusiakov, V. Tsunami History. In *The Sea*; Harvard University Press: Cambridge, MA, USA, 2009; Volume 15, pp. 23–53, ISBN 9780674031739.
3. Maramai, A.; Brizuela, B.; Graziani, L. The Euro-Mediterranean Tsunami Catalogue. *Ann. Geophys.* **2014**, *57*, S0435. [[CrossRef](#)]
4. Papadopoulos, G.A.; Gràcia, E.; Urgeles, R.; Sallares, V.; De Martini, P.M.; Pantosti, D.; González, M.; Yalciner, A.C.; Mascle, J.; Sakellariou, D. Historical and pre-historical tsunamis in the Mediterranean and its connected seas: Geological signatures, generation mechanisms and coastal impacts. *Mar. Geol.* **2014**, *354*, 81–109. [[CrossRef](#)]
5. Lorito, S.; Tiberti, M.M.; Basili, R.; Piatanesi, A.; Valensise, G. Earthquake-generated tsunamis in the Mediterranean Sea: Scenarios of potential threats to southern Italy. *J. Geophys. Res.* **2007**, *113*, B01301. [[CrossRef](#)]
6. Petricca, P.; Babeyko, A.Y. Tsunamigenic potential of crustal faults and subduction zones in the Mediterranean. *Sci. Rep.* **2019**, *9*, 1–12. [[CrossRef](#)] [[PubMed](#)]
7. Papadopoulos, G.A. *A Seismic History of Crete: Earthquakes and Tsunamis, 2000 B.C.–A.D. 2010*, 1st ed.; Ocelotos Publ.: Athens, Greece, 2011; p. 415, ISBN 978-960-9499-68-2.
8. Salamon, A.; Rockwell, T.; Ward, S.N.; Guidoboni, E.; Comastri, A. Tsunami hazard evaluation of the eastern Mediterranean: Historical analysis and selected modeling. *Bull. Seismol. Soc. Am.* **2007**, *97*, 705–724. [[CrossRef](#)]
9. Papadopoulos, G.A. *Tsunamis in the European-Mediterranean Region: From Historical Record to Risk Mitigation*; Elsevier: Amsterdam, The Netherlands, 2016; p. 271, ISBN 9870124202245.
10. Tinti, S.; Merriman, P.A.; Browitt, C.W.A. The Project GITEC: A European effort to address tsunami risk. In *Natural Disasters: Protecting Vulnerable Communities*; Th. Telford: London, UK, 1993; pp. 147–155, ISBN 978-0-7277-4835-5.
11. Papadopoulos, G.A.A. A tsunami warning system in the SW Aegean Sea, Greece. In *Early Warning Systems for Natural Disaster Reduction*; Zschau, J., Küppers, A.N., Eds.; Springer: Berlin, Germany, 2003; pp. 549–552, ISBN 978-3-642-63234-1.
12. Bocchini, G.M.; Novikova, T.; Papadopoulos, G.A.; Agalos, A.; Mouzakiotis, E.; Karastathis, V.; Voulgaris, N. Tsunami Potential of Moderate Earthquakes: The July 1, 2009 Earthquake (Mw 6.45) and its Associated Local Tsunami in the Hellenic Arc. *Pure Appl. Geophys.* **2020**, *177*, 1315–1333. [[CrossRef](#)]
13. Heidarzadeh, M.; Necmioglu, O.; Ishibe, T.; Yalciner, A.C. Bodrum–Kos (Turkey–Greece) Mw6.6 earthquake and tsunami of 20 July 2017: A test for the Mediterranean tsunami warning system. *Geosci. Lett.* **2017**, *4*, 31. [[CrossRef](#)]
14. Tinti, S.; Graziani, L.; Brizuela, B.; Maramai, A.; Gallazzi, S. Applicability of the Decision Matrix of North Eastern Atlantic, Mediterranean and connected seas Tsunami Warning System to the Italian tsunamis. *Nat. Hazards Earth Syst. Sci.* **2012**, *12*, 843–857. [[CrossRef](#)]
15. Richter, C.F. An instrumental earthquake scale. *Bull. Seismol. Soc. Am.* **1935**, *25*, 1–32.
16. Vaněk, J.; Kárník, V.; Zátonek, A.; Kondorskaya, N.V.; Riznitcenko, J.V.; Savarensky, E.I.; Solovev, S.L.; Shebalin, N.V. Standardizacija škaly magnitude (Standardization of magnitude scales). *Izvest. Acad. Sci. USSR Geophys. Ser.* **1962**, *2*, 153–158.

17. Hanks, T.C.; Kanamori, H. A moment magnitude scale. *J. Geophys. Res. Solid Earth* **1979**, *84*, 2348–2350. [[CrossRef](#)]
18. Papadopoulos, G.A.; Imamura, F.; Nosov, M.; Charalampakis, M. Tsunami magnitude scales. In *Geological Records of Tsunamis and Other Extreme Waves*, 1st ed.; Engel, M., Pilarczyk, J., May, S.M., Brill, D., Garrett, E., Eds.; Elsevier: Amsterdam, The Netherlands, 2020; pp. 33–45, ISBN 978-0-12-815686-5.
19. Abe, K. A new scale of tsunami magnitude, Mt. In *Tsunamis: Their Science and Engineering*; Iida, K., Iwasaki, T., Eds.; TERRAPUB: Tokyo, Japan, 1983; pp. 91–101, ISBN 978-94-009-7174-5.
20. Papadopoulos, G.A.; Imamura, F. A proposal for a new tsunami intensity scale. In Proceedings of the 20th International Tsunami Conference, Seattle, WA, USA, 7–10 August 2001; pp. 569–577.
21. Dogan, G.G.; Annunziato, A.; Papadopoulos, G.A.; Guler, H.G.; Yalciner, A.C.; Cakir, T.E.; Sozdinler, C.O.; Ulutas, E.; Arikawa, T.; Suzen, M.L. The 20th July 2017 Bodrum–Kos Tsunami Field Survey. *Pure Appl. Geophys.* **2019**, *176*, 2925–2949. [[CrossRef](#)]
22. Yahav, A. Israel's National Preparedness for Tsunami. International Preparedness and Response to Emergencies and Disasters-IPRED V, Abstract eBook 2018, p. 65. Available online: <http://www.ipred.co.il/wp-content/uploads/2018/01/IPRED-V-eBook.pdf> (accessed on 20 July 2020).
23. Salamon, A.; Rosen, D.S.; Gitterman, Y.; Yahav, A.; Ben-Arieh, S.; Debutton, Y.; Dover, D.; Vatenmacher, M.; Miloh, T. *Recommendations on the Policy, Warning Principles and Frame of Preparedness for Tsunamis in Israel*; Geological Survey of Israel Report; The Scientific Committee for Formulating Policy of Early Warning Principles for Tsunami Hazards in Israel: Jerusalem, Israel, 2014; In Hebrew, English abstract.
24. Papadopoulos, G.A.; Annunziato, A.; Yalciner, A.C.; Agalos, A.; Charalampakis, M.; Dogan, G.G.; Necmioglu, O.; Sozdinler, C.O.; Novikova, T.; Probst, P. The east Aegean Sea seismic tsunamis of 12 June and 20 July 2017: Lessons learned for the tsunami potential and the early warning in the Mediterranean. In *Geophysical Research Abstracts 20, Proceedings of the EGU General Assembly 2018*; European Geosciences Union: Vienna, Austria, 2018; p. 17349.
25. Cirella, A.; Romano, F.; Avallone, A.; Piatanesi, A.; Briole, P.; Ganas, A.; Theodoulidis, N.; Chousianitis, K.; Volpe, M.; Bozionellos, G. The 2018  $M_w$ 6.8 Zakynthos (Ionian Sea, Greece) earthquake: Seismic source and local tsunami characterization. *Geophys. J. Internat* **2020**, *221*, 1043–1054. [[CrossRef](#)]
26. Papageorgiou, A.; Tsimi, C.; Orfanogiannaki, K.; Papadopoulos, G.A.; Sachpazi, M.; Lavigne, F.; Grancher, D. Tsunami Questionnaire Survey in Heraklion Test Site, Crete Island, Greece. In *Geophysical Research Abstracts 17, Proceedings of the EGU General Assembly 2015*; European Geosciences Union: Vienna, Austria, 2015; p. 10784.
27. Cerase, A.; Crescimbene, M.; La Longa, F.; Amato, A. Tsunami risk perception in southern Italy: First evidence from a sample survey. *Nat. Hazards Earth Syst. Sci.* **2019**, *19*, 2887–2904. [[CrossRef](#)]
28. Abe, K. Estimate of tsunami run-up heights from earthquake magnitudes. In *Tsunamis: Progress in Prediction, Disaster Prevention and Warning*; Tsuchiya, Y., Shuto, N., Eds.; Kluwer: Amsterdam, The Netherlands, 1995; pp. 21–35.
29. Lekkas, E.; Andreadakis, E.; Kostaki, I.; Kapourani, E. A Proposal for a New Integrated Tsunami Intensity Scale (ITIS2012). *Bull. Seismol. Soc. Am.* **2013**, *103*, 1493–1502. [[CrossRef](#)]

